Lattice Monte Carlo Simulations of Chain Conformations in Polymer Nanocomposites

Murat S. Ozmusul and Catalin R. Picu

Department of Mechanical, Aerospace and Nuclear Engineering, Rensselaer Polytechnic Institute, Troy, New York 12180

S. S. Sternstein

Department of Materials Science and Engineering, Rensselaer Polytechnic Institute, Troy, New York 12180

Sanat K. Kumar*

Department of Chemical and Biological Engineering, Rensselaer Polytechnic Institute, Troy, New York 12180

Received December 8, 2004; Revised Manuscript Received February 25, 2005

ABSTRACT: Lattice Monte Carlo simulations were performed on monodisperse polymer melts, with DP's ranging from 100 to 400, filled with nanoparticles of sizes comparable to the chain R_g. We critically study the role of the mean distance between these nanofillers on the overall conformation of polymer chains and, more importantly, on the statistics of bridges, dangling ends, loops, and trains. We are motivated to study these issues since it has been suggested that the mechanical behavior of nanocomposites result from the formation of a long-lived transient filler network mediated by the chains. Further, the experimentally observed increase in low frequency, low strain amplitude elastic modulus on the addition of filler is attributed to strongly stretched bridge segments. We find that the overall chain statistics remain Gaussian regardless of filler loading (up to 27 vol %). Short bridges, loops, and tails are strongly stretched, but in a manner that is quantitatively equivalent to the statistics of subchains in a melt. These results unequivocally assert that nanoparticles do not affect equilibrium melt chain conformations and that this idea can underpin the development of new models for polymer nanocomposites.

1. Introduction

Polymer-based nanocomposites are of great current interest since it has been found that the addition of nanoparticles in some cases could significantly enhance the stiffness and strength of polymer matrices as compared to property enhancements achieved with micron-sized fillers at the same loading e.g., ref 1. Similarly, ductility, and toughness can be enhanced without loss of strength,[1,2] scratch resistance improved,[2] and rubbery behavior obtained from a filled relatively brittle polymer.[3] Experiments have conclusively demonstrated[4−7] that the interesting mechanical properties of nanocomposites result when (a) the dispersion of nanoparticles in the polymer matrix is good and (b) the filler spacing is such that the average wall-to-wall distance between neighboring particles becomes comparable to the unperturbed chain dimensions. Recent simulations support the idea that a polymer-mediated transient network of filler, i.e., a filler connected by polymer, where the filler and polymer interact through the formation of physical bonds,[8−10] would explain these experimental results. This network should form when fillers are "sufficiently close", i.e., when the wall-to-wall distance is of the order of several chain gyration radii (R_g). The intuitive appeal of this theory is high, but quantitative predictions that may be compared with experimental results require a thorough understanding of the structure and dynamics of chains confined between spherical fillers. However, a crucial issue is the extremely high reinforcement (ratio of composite modulus to neat polymer modulus) that is obtained at relatively low filler concentrations (ca. less than 10 vol %), this reinforcement being as much as 30 times what is predicted from simple mixing (micromechanical) theory. In an attempt to explain this extraordinary level of reinforcement by nanofillers, Sternstein and Zhu[6,11] have proposed that Langevin chain statistics are a major contributor to stiffening of the matrix and hence the composite. The objective of this work is to provide further insight into this issue.

The structure of linear monodisperse polymeric chains in the vicinity of flat surfaces has been studied by analytical theories and computer simulations[12−21] and by experiment.[22,23] It has been found that chains do not distort even when they are confined into films as thin as R_g. Rather, they will orient their long axes parallel to the surfaces so as to minimize any conformational distortion of the chains. In contrast to these established ideas, recent studies on the conformation of polymer chains in the presence of curved nanoparticles are controversial. Mark and collaborators[24,25] performed simulations of phantom (or Gaussian) chains in the presence of a prescribed volume fraction of impenetrable spheres. The chains are found to either stretch or compress, depending on the ratio of the chain dimension and the mean wall-to-wall distance. Experimental results published by Nakatani et al.[26] appear to support these conclusions. However, recent Monte Carlo[27−30] and molecular dynamics[31] simulations of melts of self-avoiding chains in the presence of filler show that chain dimensions are always smaller compared to the bulk at high and moderate filler volume fractions. At low

* Corresponding author. E-mail: kumar@rpi.edu.

10.1021/ma0474731 CCC: $30.25
Published on Web 04/15/2005

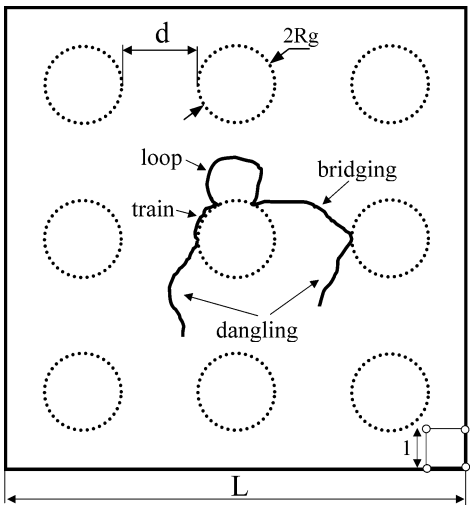

Figure 1. Schematic 2-D representation of the 3-D model used in our simulations.

volume fractions of filler the chains are not distorted, consistent with the results obtained from the polymer melts near flat surfaces. Vacatello persuasively argues[32] that the assumption of noninteracting chains made in refs 24 and 25 is not valid for filled systems and that melts of self-avoiding chains at proper densities have to be modeled if a clear understanding of chain conformations is to be obtained.

While these studies have focused on chain scale structure, our interest is in the structure of chains that participate in the polymer-mediated transient network between the filler particles.[10] We consider systems with three different filler volume fractions ($\leq$27%) as representative of experimentally studied nanocomposites. The wall-to-wall distance is selected to be on the order of the chain size ($0.5R_g$, R_g, and $2R_g$), while the radius of the spherical fillers is taken to be $\sim R_g$. The overall conformations of the chains are found to follow Gaussian statistics, suggesting that the filler particles only cause minor perturbations at this scale. The statistics of subchain segments with a small number of monomers (i.e., bridges, dangling segments, loops, and trains) are strongly non-Gaussian, especially for the highest filler loadings. However, these results are quantitatively equivalent to the statistics of subchains in an unfilled melt, suggesting that the presence of particles barely affects chain conformations, apparently on any scale. These results are consistent with experimental results on filled polymers[6] and appear to thus provide a good starting point for the development of theories to describe the mechanical properties of these composites.[33] It is important to emphasize that the chain conformations studied in this work represent static snapshots of the systems, implying that we do not account for the temporal persistence of the network: such temporal effects are conjectured to be critical in determining the frequency-dependent mechanical properties of these materials.[9]

2. Modeling and Simulation Procedure

We performed Metropolis Monte Carlo (MC) simulations on simple cubic lattices with bond lengths varying between 1 and $\sqrt{3}$ (i.e., a coordination number of $z = 26$). Periodic boundary conditions are imposed in all three directions. A 2-D projection of the 3-D simulation cell is schematically shown in Figure 1 with a unit cell of the lattice being sketched in the right lower corner. The cell contains 27 fillers placed in a simple cubic configuration. We have also considered fillers which are placed at random in the simulation cell: since the results obtained from the ordered and disordered matrices are similar, we only present the results from the ordered matrices here. The rationale for the lack of sensitivity to filler placement is addressed in the Discussion section. The spherical filler particles are first placed in the simulation box, and the sites occupied by these filler particles are defined as forbidden sites to monomers. Because of the way they are defined, the surface of the fillers have a roughness reflective of the underlying lattice. The fillers are stationary during the simulation. After the fillers are placed in the box, the system of self-avoiding chains of length N are placed on the lattice until the desired bead number density, ρ, is achieved. The chains are monodisperse, with lengths of $N = 100$, 200, and 400 in separate simulations. The excluded-volume condition is strictly enforced at all times, each lattice site being occupied by at most one bead. No bond potential is considered, and there are no attractive interactions between any two polymer beads. Dense systems corresponding to polymer melts are considered, with the number density ρ being 0.75. The polymer density is evaluated relative to the volume available to the polymers. When changing the chain length, all dimensions of the system scale accordingly (with R_g) while keeping the volume fraction unchanged. The parameters of our simulations (namely box size, L, chain length, N, the filler diameter, D_f, and the number of filler considered, N_f) are shown in Table 1.

Energetic interactions between polymeric chains and fillers are imposed through a square potential well of depth w. The well extends over the nearest $z = 26$ lattice sites, i.e., a distance of $\sqrt{3}$ lattice spacings from the surface of each filler. The polymer−filler affinity is controlled by the depth of the well, w. Weak, moderate, and strong values of the affinity parameter, i.e., $w = 0.2kT$, $2kT$, and $10kT$, respectively, were employed in a series of simulations.

After the initial structure of the nanocomposite is created, the equilibration process starts. Only local moves, i.e., moves to immediate nearest neighbors, are made. Addition of reptation moves and configurational biased moves would help to rapidly equilibrate the sample, but we only use local moves in the production phase so as to track the mobility of the chains in the system. The moves are accepted following the standard Metropolis criterion. In the case of a pure melt with no filler, this criterion simplifies to accepting any move that does not induce an overlap of two beads. Following the well-established results of Binder and co-workers, the diffusion of beads and center of mass of the chains were monitored, and the equilibration phase was run until the mean displacement of the center of mass is on the order of the chain size. This occurred after 10 million Monte Carlo steps (MCS) in the $N = 100$ system. Here, one MCS corresponds to N_cN move attempts, i.e., one move attempt per bead. The same algorithm is employed for the production phase. The polymer structure is obtained by averaging over time (MCS) and over a number of replicas of the system in order to reduce the statistical noise. The production phase was run for about 30 million MCS, and the results were averaged over 10

Table 1. Parameters of Our Simulations

wall-to-wall distance, d	simulation cell size, L	chain length, N	no. of chains, N_c	no. of filler, N_f	filler diameter, D_f	wall interaction, w
$^1/_2R_g$	51	100	756	27	12	$10kT$
R_g	59	100	1264	27	12	$10kT$
$2R_g$	73	100	2550	27	12	$10kT$
$^1/_2R_g$	51	100	756	27	12	$2kT$
R_g	59	100	1264	27	12	$2kT$
$2R_g$	73	100	2550	27	12	$2kT$
$^1/_2R_g$	51	100	756	27	12	$0.2kT$
R_g	59	100	1264	27	12	$0.2kT$
$2R_g$	73	100	2550	27	12	$0.2kT$
R_g	77	200	1400	27	16	$2kT$
$2R_g$	99	200	3200	27	16	$2kT$
R_g	115	400	2324	27	24	$2kT$
$2R_g$	149	400	5454	27	24	$2kT$

independent replicas of the system. The replicas are statistically uncorrelated, each being a totally new realization of the system.

3. Results

3.1. Overall Chain Conformation. The distribution of the RMS end-to-end vector is shown in Figure 2 for $d = {}^1/_2R_g$, $d = R_g$, and $d = 2R_g$. The neat polymer case is also shown for reference. The curves are identical for the three different filler loadings, suggesting that the overall conformations of the chains follow Gaussian statistics. This conclusion is consistent with recent findings of Vacatello, who, as in our work, simulated self-avoiding chains at meltlike densities in the presence of filler.[24,25,28,30,32] Presumably, we have to consider even higher filling fractions to see measurable differences in chain statistics between the filled systems and the bulk melts.

3.2. Bridges. The importance of bridges derives from the fact that they are central to the formation of a transient particle network. Additionally, if the lifetime of this network is long enough, the stiffness of the composite should increase dramatically. Figure 3 shows the distribution of number of monomers in a bridge. There are three sets of curves, corresponding to $d = {}^1/_2R_g$, R_g, and $2R_g$. For each given d value (say R_g), the ratios d/R_g and d/particle size are chosen to be independent of N. Since the distribution of bridge lengths (Figure 3) is also independent of N in these studies, we conclude that our results correspond to the polymeric limit. The effect of the affinity parameter, w, that describes the strength of the polymer−filler attraction ($w = 10kT$, $2kT$, $0.2kT$) is weak in this context; w perturbs the local polymer configuration, in the vicinity of the wall, but not the longer ranged structure. Thus, both the mean number of monomers in a bridge and their end-to-end distances are hardly affected by w. Similar results are also found for tails, loops, and trains (as discussed below), and hence, in all future discussion we shall use $w = 2kT$ and not consider any variations in this variable. However, it is emphasized that filler−polymer bond strength is known to be a primary variable in determining the reinforcement levels[6] and the recovery kinetics of modulus following large strain applications,[11] both of which correspond to dynamic quantities not considered in this work.

The total number of bridging segments per filler depends strongly on the wall-to-wall distance, d. For $N = 100$, we find for $d = R_g$ that 8% of lattice sites (65 out of 830) on a particle surface are associated with polymer bridges. When the wall-to-wall distance d increases to $2R_g$, the total number of bridging segments per filler decreases to 17 (2% of the available sites on the filler

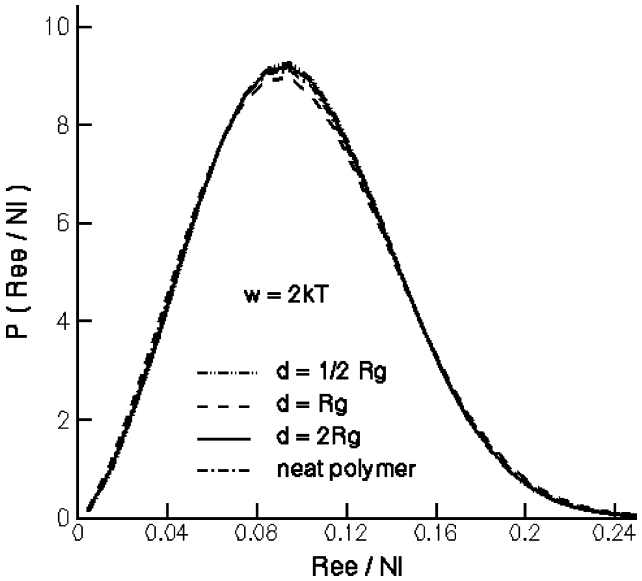

Figure 2. Distribution of the RMS end-to-end vector length of chains in the unfilled polymer and in filled systems with $d = {}^1/_2R_g$, $d = R_g$, and $d = 2R_g$, $N = 100$, and $w = 2kT$.

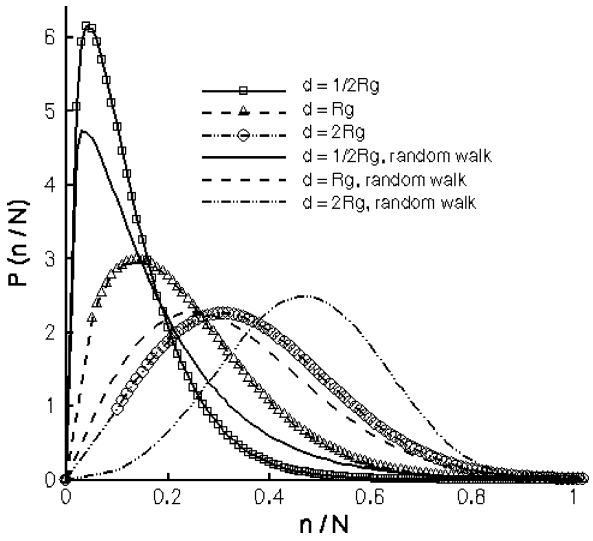

Figure 3. Probability density distribution function of the normalized number of bonds in a bridging segment for systems with wall-to-wall distance $d = {}^1/_2R_g$, R_g, and $2R_g$, $w = 2kT$, and chain length $N = 100$, 200, and 400. The distribution of the normalized number of bonds in a bridge segment is independent of the chain length N. Note that data from SAW chains and phantom chains are shown in this plot.

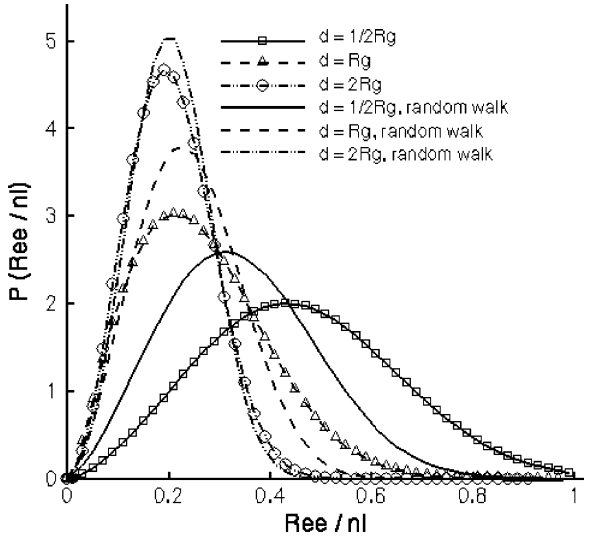

Figure 4. Probability density distribution function of the ratio of the RMS end-to-end vector length to the number of chain segments in a bridge for systems with wall-to-wall distance $d = {}^1/_2R_g$, R_g, and $2R_g$, $w = 2kT$, and chain length $N = 100$. Note that data from SAW chains and phantom chains are shown in this plot.

surface). We expect this number to decrease continually with increasing d, suggesting that the probability of the creation of a transient network decreases dramatically with increasing d.

Figure 4 shows the probability density function (PDF) of the ratio of the RMS end-to-end distance of a bridge to the number of monomers in a bridge, n, times l, the lattice spacing. (l is smaller than the mean bond length, which turns out to be $\sim 1.62l$.) We plot the data in this form to critically examine the deformation of these bridges relative to the ideal, Gaussian state. It is clear that, with decreasing d, there is an increased propensity for more stretched bridges. This is simply a consequence of the increased number of short bridges as the particle separation is decreased.

3.3. Dangling Segments (Tails). A large number of dangling segments are attached to each filler. As in the case of bridges, an attachment point is defined when a bead resides in a layer of unit thickness at the surface of a filler. About 10% of the filler surface sites are occupied by dangling segments. The PDF of the number of bonds in a dangling segment is shown in Figure 5a for $d = {}^1/_2R_g$, R_g, and $2R_g$ and for all three chain lengths considered. With decreasing d there are more short segments due to the fact that when the wall-to-wall distance is a small fraction of the chain size, dangling segments become bridges. The PDF of the ratio of the RMS end-to-end distribution to the length of a dangling segment is shown in Figure 5b. Again, with decreasing d values there is an increased fraction of stretched dangling ends, reflecting the increased probability of finding short dangling ends with decreasing d (Figure 5a).

3.4. Loops. A dense population of loops exists on the surface of each filler. Loop ends occupy about 37% of the available surface sites. The total number of loops per filler particle and therefore their surface coverage are independent of d. The distribution of number of bonds in a loop is shown in Figure 6. The most important observation here is that most of the loops are very short and that, to first order, the loop distribution (plotted against n, not n/N) is independent of d and

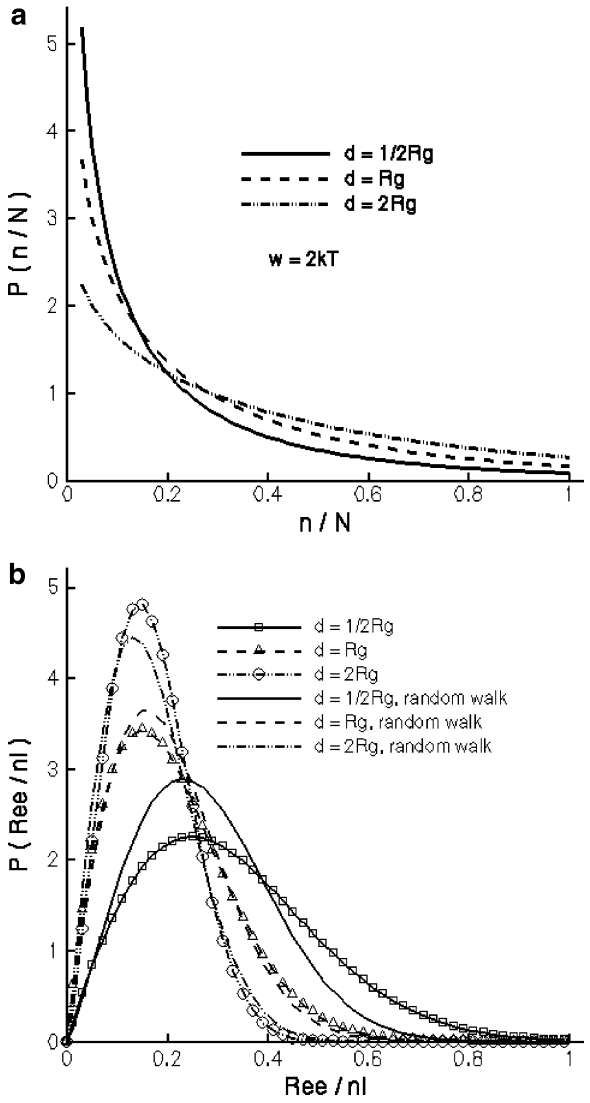

Figure 5. (a) Probability density distribution function of the normalized number of bonds in a dangling segment for systems with wall-to-wall distance $d = {}^1/_2R_g$, R_g, and $2R_g$, with chain length $N = 100$ and filler affinity $w = 2kT$. The distribution is independent of the chain length. (b) Probability density distribution function of the ratio of the RMS end-to-end vector length to the number of segments in the tails for systems with wall-to-wall distance $d = R_g$ and $2R_g$, with chain length $N = 100$, 200, and 400 and filler affinity $w = 2kT$. Data are also shown for $d = {}^1/_2R_g$, but only for $N = 100$. Note that data from SAW chains and phantom chains are shown in both plots.

chain length. A more careful examination shows that there is small decrease in mean loop length with decreasing d, consistent with the results found for the dangling tails.

3.5. Trains. A large number of train segments exist. These are chain segments longer than one bond length (two beads) that are snaking on the surface of the filler without a single monomer leaving the surface. The trains are essentially inactive in stress production. Their importance is associated with the detachment process. During deformation, when an chain segment is pulled from the wall, the presence of a long train makes it harder to detach this segment and take it away from the surface. The lifetime of these trains therefore increase due to this cooperativity. Therefore, the trains contribute to defining the strain rate sensitivity of the composite. As shown in Figure 7, the trains may be as long as 10 bonds, although the probability of such

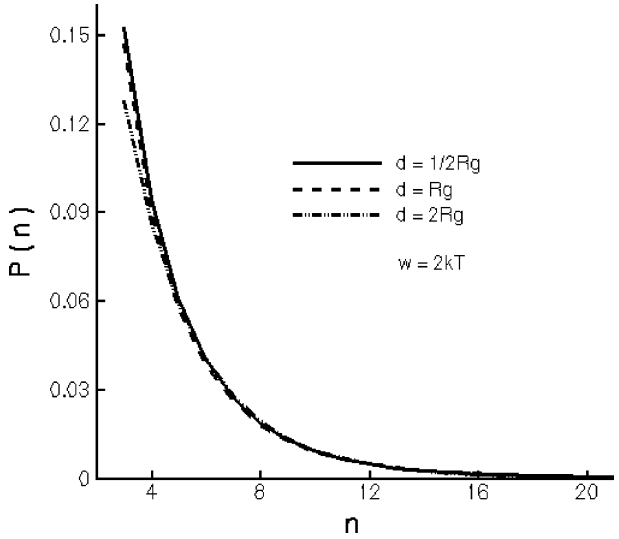

Figure 6. Probability density distribution function of the number of bonds in a representative loop segment for systems with $d = {}^1/_2R_g$, R_g, and $2R_g$, $N = 100$, and polymer−filler affinity $w = 2kT$.

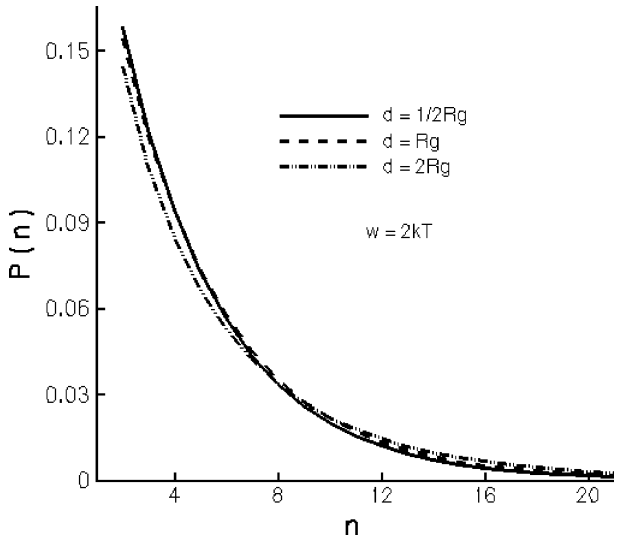

Figure 7. Probability density distribution function of the number of bonds in a train in systems with $d = {}^1/_2R_g$, R_g, and $2R_g$, filler affinity $w = 2kT$, and chain length $N = 100$. The distribution is weakly affected by the wall-to-wall distance.

entities is small. Most trains are 2−4 bonds in length. The data presented in the figure suggest that the average train length is not a function of chain length or of the wall-to-wall distance, d.

4. Discussion

Our major focus in this paper is to understand the behavior of loops, bridges, dangling ends, and trains that form the transient filler network mediated by favorable polymer surface interactions. While we have discussed these results above, it is important to understand these findings in the context of well-developed models familiar to polymer scientists. Sternstein and Zhu[6,11] argue that the mechanical reinforcement that is afforded by the filler is due to the presence of highly stretched bridge segments which assume Langevin statistics. To carefully assess the applicability of Gaussian chain statistics to the distribution of loops, bridges, etc., we have conducted two new series of simulations. The first set of calculations closely track the simulations presented

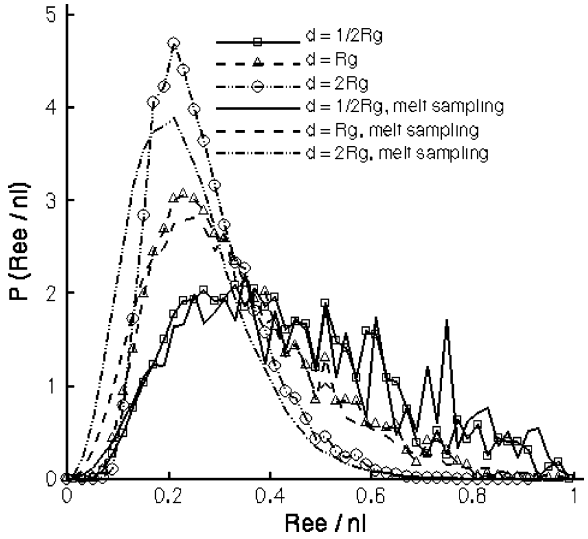

Figure 8. Probability density distributionof the normalized number of bonds in a bridging segment for systems with wall-to-wall distance $d = {}^1/_2R_g$, R_g, and $2R_g$, $w = 2kT$, and chain length $N = 100$.

in section 2, except that the excluded-volume criterion between two polymer segments is turned off. Thus, the chains immediately get transformed into phantom (presumably Gaussian) objects, which, however, experience excluded-volume interactions with the filler. The results of these calculations are shown in Figures 3−5.

Let us focus first on bridges. It is clear that the phantom Gaussian chain simulations predict a much larger value of the mean number of monomers in a bridge. Similarly, the distribution of bridge lengths (Figure 3) is skewed to large (n/N) values for the phantom chains. These effects become more pronounced with decreasing d. We suggest that these findings stress the simple fact that self-avoiding chains are stiffer than phantom chains. When we consider the distribution function for the ratio of the RMS end-to-end distance to the number of segments in a bridge (Figure 4) or in a dangling end (Figure 5b), it is clear that for $d = 2R_g$ the distribution functions for both the phantom chains and self-avoiding chains almost overlap. These results stress that for large filler separations the bridges are long enough to assume a Gaussian distribution. For smaller filler separations, however, it is clear that the self-avoiding simulations are clearly biased to more stretched conformations, consistent with the notion that these chains are stiffer and hence correspond to a higher value of R_{ee}/nl (relative extension ratio). Note that the bridges appear to be in less agreement with Gaussian statistics than the loops, especially for $d = R_g$.

While these results are interesting, perhaps more relevant are a second series of calculations. We begin with the distribution of the number of monomers in a bridge, $P(n)$, shown in Figure 3. We now examine a monodisperse melt of chains of length $N = 100$ and study the end-to-end distance for chain fragments which have the same distribution of the number of monomers as the bridges. (We still consider a monodisperse melt but only examine the statistics of subchains of the right length in frozen snapshots.) Such calculations are then used to generate the probability distribution function for the quantity, R_{ee}/nl, also examined in Figure 4. Figure 8 shows the resulting probability distributions for the three different values of particle separation considered in the simulations. The results of this

analysis are somewhat surprising. For large extensions, i.e., for $R_{ee}/nl \rightarrow 1$, it is clear that the results from the filled systems and the melts practically superpose. These results, which apply for all three filler loadings, unequivocally assert that the large chain stretching limit is purely a consequence of the self-avoidance of short chain fragments and that this result is unaffected by the addition of filler particles to the melt. Similar results are obtained for all smaller extensions, all the way down to the peak in the distribution. In the other limit, namely $R_{ee}/nl \rightarrow 0$, it is clear that the melt results overpredict the results obtained from the filled systems. This result merely reflects the fact that two ends of a bridge segment, which fall on different particles by construction, cannot be at the same location in space. This result, therefore, merely reflects the uniqueness of our definition of a bridge but does not reflect any breakdown in the statistics of chain conformations. In summary, therefore, short bridge (and loops and tails) segments are stretched relative to their Gaussian analogues, but only in a manner that is consistent with the behavior of an unfilled melt.

Finally, we remark briefly on our finding that the spatial ordering of fillers (i.e., ordered vs random) does not affect the results obtained for bridge extension distributions. Our results, which suggest that the extensions of bridges, loops, and tails are consistent with melt statistics, clearly suggest that the placement of filler particles cannot be relevant in this context. In contrast, we expect that the distributions of monomers in a bridge (or loops, bridges) will be somewhat different depending on the spatial distribution of nanoparticles.

5. Conclusions

The static structure of polymeric chains in a polymer nanocomposite filled with nanoparticles was investigated by means of MC lattice simulations. Our results, taken in composite, support the notion that the mechanical reinforcement afforded by addition of filler occurs due to the creation of a polymer-mediated transient network between the filler particles. The transient network possesses more connectivity between the particles with increasing filler content since the mean distance between fillers decreases. In addition, on increasing filler content, there is a larger fraction of strongly stretched chain segments which make up bridges. In all these cases the chains essentially retain their meltlike conformations in the nanocomposites, consistent with the notion that it is hard to distort chains in a melt. More simulations are necessary to elucidate the dynamic properties of these networks, especially focusing on the role of the affinity parameter, w, which is expected to critically determine the lifetime of these transient networks and hence the dependence of mechanical properties on strain amplitude and history.

Acknowledgment. This work was supported in part by the Office of Naval Research through Grant N00014-01-1-0732 and by the National Science Foundation (Multiscale Systems Engineering for Nanocomposites, CMS-0310596).

References and Notes

(1) Petrovic, Z. S.; Javni, I.; Waddon, A. *Proc. ANTEC* **1998**, 2390.
(2) Ng, C.; Schadler, L. S.; Siegel, R. W. *J. Nanostruct. Mater.* **1999**, *12*, 507.
(3) Ash, B. J.; Rogers, D. F.; Wiegand, C. J.; Schadler, L. S.; Siegel, R. W.; Benicewicz, B.; Apple, T. *Polym. Comput.* **2002**, *23*, 1014.
(4) Vollenberg, P. H. T.; Heikens, D. *Polymer* **1989**, *30*, 1656.
(5) Vollenberg, P. H. T.; deHaan, J. W.; van de Ven, L. J. M.; Heikens, D. *Polymer* **1989**, *30*, 1663.
(6) Sternstein, S. S.; Zhu, A. J. *Macromolecules* **2002**, *35*, 7262.
(7) Mitchell, C. A.; Bahr, J. L.; Arepalli, S.; Tour, J. M.; Krishamoorti, R. *Macromolecules* **2002**, *35*, 8825.
(8) Reichert, W. F.; Goritz, D.; Duschl, E. J. *Polymer* **1993**, *34*, 1216.
(9) Salaniwal, S.; Kumar, S. K.; Douglas, J. F. *Phys. Rev. Lett.* **2002**, *89*, 258301.
(10) Vacatello, M. *Macromol. Theory Simul.* **2003**, *12*, 86.
(11) Zhu, A.; Sternstein, S. S. *Compos. Sci. Technol.* **2003**, *63*, 1113.
(12) Sen, S.; Cohen, J. M.; McCoy, J. D.; Curro, J. G. *J. Chem. Phys.* **1994**, *101*, 9010.
(13) de Gennes, P. G. *Adv. Colloid Interface Sci.* **1987**, *27*, 189.
(14) Scheutjens, J. M. H. M.; Fleer, G. J. *J. Phys. Chem.* **1979**, *83*, 1619.
(15) Scheutjens, J. M. H. M.; Fleer, G. J. *Macromolecules* **1985**, *18*, 1882.
(16) Zhan, Y.; Mattice, W. L. *Macromolecules* **1994**, *27*, 7056.
(17) Mansfield, K. F.; Theodorou, D. N. *Macromolecules* **1991**, *24*, 6283.
(18) Kumar, S. K.; Vacatello, M.; Yoon, D. Y. *Macromolecules* **1990**, *23*, 2189.
(19) Yethiraj, A. *J. Chem. Phys.* **1994**, *101*, 2489.
(20) Eisenriegler, E.; Kremer, K.; Binder, K. *J. Chem. Phys.* **1982**, *77*, 6296.
(21) Bitanis, I. A.; ten Brinke, G. *J. Chem. Phys.* **1993**, *99*, 3100.
(22) Jones, R. L.; Kumar, S. K.; Ho, D. L.; Briber, R. M.; Russell, T. P. *Nature (London)* **1999**, *400*, 146.
(23) Kraus, J.; Muller-Buschbaum, P.; Kuhlmann, T.; Schubert, D. W.; Stamm, M. *Europhys. Lett.* **2000**, *49*, 210.
(24) Kloczkowski, A.; Sharaf, M. A.; Mark, J. E. *Chem. Eng. Sci.* **1994**, *49*, 2889.
(25) Yuan, Q. W.; Kloczkowski, A.; Mark, J. E.; Sharaf, M. A. *J. Polym. Sci., Polym. Phys.* **1996**, *34*, 1647.
(26) Nakatani, A. I.; Chen, W.; Schmidt, R. G.; Gordon, G. V.; Han, C. C. *Polymer* **2001**, *42*, 3713.
(27) Vacatello, M. *Macromolecules* **2001**, *34*, 1946.
(28) Vacatello, M. *Macromolecules* **2002**, *35*, 8191.
(29) Ozmusul, M. S.; Picu, R. C. *Polymer* **2002**, *43*, 4657.
(30) Picu, R. C.; Ozmusul, M. S. *J. Chem. Phys.* **2003**, *118*, 11239.
(31) Starr, F. W.; Schroder, T. B.; Glotzer, S. C. *Macromolecules* **2002**, *35*, 4481.
(32) Vacatello, M. *Macromolecules* **2003**, *36*, 3411.
(33) Sarvestani, A. S.; Picu, R. C. *Polymer* **2004**, *45*, 7779.

MA0474731